

Primordial gravitational waves (GWs), observable as stochastic background with the planned Laser Interferometer Space Antenna (LISA), could be produced by magnetic fields generated at the time of the electroweak phase transition. There is the possibility that they might be helical [1, 2]. Such fields would have decayed more slowly than nonhelical ones, and would thus have a chance to survive until the present time [3] to explain the lower limits on the magnetic field strength inferred through the non-observation of secondary cascade photons with FERMI [4]. Such fields could be generated during the electroweak phase transition and would undergo forward and inverse cascading during the entire radiation era until recombination [5]. The inverse cascade manifests itself through a shift in the peak of the magnetic energy spectrum [6, 7]. The forward cascade, on the other hand, would manifest itself through the development of a steeper slope of the normalized magnetic helicity [8], so that the magnetic field is no longer fully helical at high wavenumbers, if the initial magnetic field was fully helical at all wavenumbers. This change would become evident if the development of the new slope takes a sufficient amount of time. Details of this process, including its duration, could manifest themselves in the circular polarization of the resulting GW signal. However, the magnetic field will gradually decay and its ability to contribute to the resulting GW production diminishes. This can happen rather rapidly. Therefore, whether or not it is detectable in the GW signal depends on just how rapidly the magnetic field starts to decay.

Here, we use direct numerical simulations of primordial magnetic fields together with the resulting GW production to investigate the effect of the time-dependence of the source on the GW signal. We use the PENCIL CODE [9] for these calculations, which is well suited for primordial MHD simulations and which comes with a GW solver readily available for our purposes [10]. All simulations have a resolution of  $1024^3$  meshpoints. Earlier analytic work showed that the degree of circular polarization changes with wave number if the spectral slopes of the symmetric

and antisymmetric parts of the magnetic correlation tensor are different from each other, but it stays independent of  $k$  if the spectra have the same slope [11, 12]. Those analytic calculations have made use of certain approximations, but recent numerical work [13] showed that the predictions from the analytical model regarding the degree of polarization are surprisingly well reproduced by the numerical simulations.

As we have already mentioned, the decay of the magnetic field causes a decline of the turbulent driving of GWs. This decline is further enhanced by the expansion of the universe, although this effect is small if the decay time of the turbulence is short compared with the Hubble time. Mathematically, this decline in the GW source is caused by an increase of the scale factor  $a$  that enters in the denominator of the stress term in the GW equation. Using conformal time,  $t = \int dt_{\text{phys}}/a(t_{\text{phys}})$ , and comoving strain,  $h = ah_{\text{phys}}$ , where  $t_{\text{phys}}$  and  $h_{\text{phys}}$  are physical time and strain, the linearized GW equation reads

$$(\partial_t^2 - \nabla^2) h_\lambda = 6T_\lambda/t \quad (\text{for } t \geq 1), \quad (1)$$

where  $\lambda = +$  or  $\times$  denote the plus or cross polarization modes, which are the two independent tensor modes compatible with the Einstein equations, and the  $T_\lambda$  are the sums of Reynolds and Maxwell stresses, projected onto the  $\lambda = +$  or  $\times$  modes.

For a fully helical magnetic field, the magnetic energy, and thus also the magnetic stress decay like  $T_\lambda \sim (t-1)^{-2/3}$ ; see [14] for a corresponding result in ordinary MHD, and Refs. [3, 15] for applications in the cosmological context. For  $t \ll 2$ , this effect is clearly more important than that of the cosmological expansion, which will nevertheless be retained in our simulations.

The authors of Ref. [16] considered two types of simulations; (i) one where the initial turbulence spectrum is *given* and (ii) one where the magnetic energy spectrum is *driven* by the injection of an electromotive force. Their direct numerical simulations showed that when the initial turbulence spectrum is given, the degree of circular polarization

is independent of the wave number for  $k > 2k_*$ , where  $k_*$  is the wave number of the energy-carrying scale of the turbulence, i.e., where the magnetic energy spectrum peaks. On the other hand, when the magnetic energy spectrum is driven, the degree of circular polarization declines to zero with increasing value of  $k$ . Based on the model of Ref. [11], this can be understood as a consequence of the fact that with a given initial spectrum, the magnetic field is fully helical at all wave numbers, and only at late times a decline of the degree of circular polarization of GW could be expected when the current helicity cascade of the magnetic field gets established and  $kH_M(k)$  becomes steeper than  $E_M(k)$  for  $k > 2k_*$ . To test this idea in detail, we must consider different time dependencies of the magnetic field. This cannot be done in a fully self-consistent model, where the decay law is always fixed.

To model a slow-down in the decay, we could “modify” the MHD equations. For example, if the induction equation is dominated by the Hall effect, the magnetic energy decay is slower and becomes proportional to  $\sim t^{-2/5}$ . However, to have a more controlled experiment, we now consider solutions of the GW equation where the source term on the right-hand side is scaled by a time-dependent factor,  $F(t)$ , i.e.,

$$T_\lambda(\mathbf{x}, t) \rightarrow F(t) T_\lambda(\mathbf{x}, t). \quad (2)$$

We consider two possibilities. In models of type A, we compensate or even overcompensate for the decay of the magnetic field. Note, however, that we preserve the natural temporal fluctuations and the intrinsic changes of the spectra, including changes in the location of the peak due to the forward and inverse cascades, respectively. To an excellent approximation, the decay of a helical field can be modeled as

$$\mathcal{E}_M = \mathcal{E}_{M0}/[1 + (t - 1)/\tau]^{2/3}. \quad (3)$$

For the fully helical simulation of Ref. [16], which is the fiducial model for the experiments presented here, we find  $\mathcal{E}_{M0} = 0.0031$  and  $\tau = 0.053$ . In that case, we choose  $F(t) = [1 + (t - 1)/\tau]^n$  and vary the value of  $n$ . For  $n = 2/3$ , the overall amplitude of the effective stress stays constant, while for  $n > 2/3$ , the decay is overcompensated, so we expect an accelerated growth of the GW energy.

As we will see below, when  $n = 2/3$ , the effect on the growth of GW energy is very weak, because the resulting GW amplitude depends decisively on the

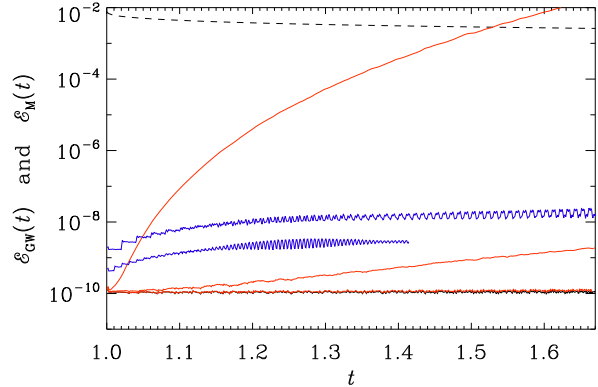


Figure 1: Normalized GW and magnetic energies versus time for models of type A (red) and B (blue). The black solid and dashed lines refer to GW and magnetic energies for  $F(t) = 1$ .

temporal variation of the source at later times. To boost the effective temporal frequency of the signal, we also consider a model where we give regular instantaneous “kicks” to the amplitude of the stress. This corresponds to a staircase profile for the scaling factor  $F(t)$  in front of the stress term, i.e.,

$$F(t) = 1 + \epsilon \sum_{m=1}^{\infty} m\theta(t - m\tau), \quad (4)$$

where  $\epsilon$  determines the slope of the increase of  $F(t)$ ,  $\tau$  is the interval of kicks (here  $\tau = 0.05$ ), and  $\theta(t) = 1$  for  $t > 0$  and 0 otherwise is the Heaviside step function.

In Figure 1, we present results for the energy evolution for different values of  $n$  for models of type A and for different combinations of  $\epsilon$  and  $\tau$  for models of type B. In all cases, there is a statistically monotonous increase of  $\mathcal{E}_{GW}$ . We emphasize that the GW energies obtained for models with  $F(t) \gg 1$  reach obviously unrealistically large values, which is necessary to show that the magnetic influence very quickly becomes negligible in all realistic situations.

Next, we consider for different times magnetic and GW energy spectra,  $E_M(k)$  and  $E_{GW}(k)$ , respectively. They are normalized such that  $\int E_M(k) dk = \mathcal{E}_M$  and  $\int E_{GW}(k) dk = \mathcal{E}_{GW}$ . Occasionally, we also use the GW energy per logarithmic wavenumber interval,  $\Omega_{GW}(k) \equiv kE_{GW}(k)$ . We see that at early times, the spectra of  $2E_M(k)$  and  $kH_M(k)$  coincide, as required by the realizability condition for a fully helical magnetic field [17].

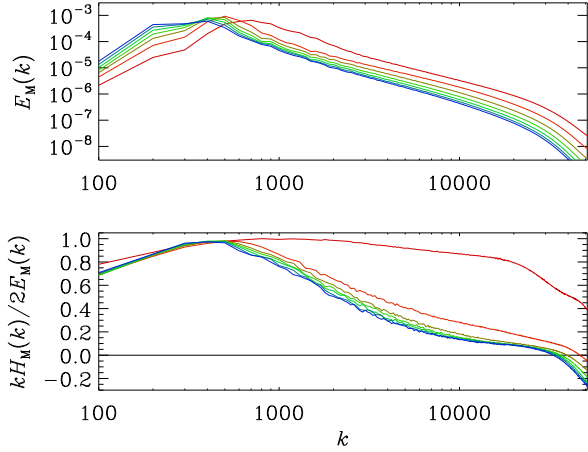


Figure 2: Magnetic energy spectra (upper panel) and fractional magnetic helicity spectra (lower panel) at  $t = 1.01, 1.1, 1.2, \dots, 1.6$ , marked by colors ranging from red to green and blue, for the fully helical run of Ref. [16].

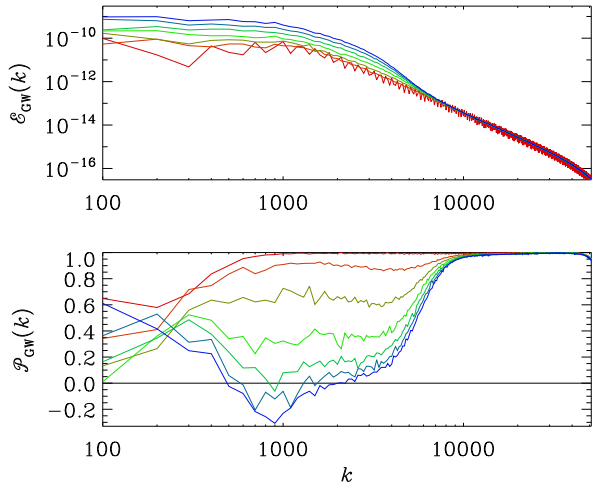


Figure 3: GW energy (upper panel) and degree of polarization (lower panel) at the same times as in Figure 2 for a model of type A with  $n = 2$ .

At late times, however, the current helicity, whose spectrum is proportional to  $k^2 H_M(k)$ , displays a forward cascade with a slope proportional to  $k^{-5/3}$ , which implies a  $k^{-8/3}$  spectrum for  $E_{GW}(k)$ ; see Ref. [13].

For small values of  $n$ , the GW spectrum displays at all times the same spectrum for  $\Omega_{GW}(k) \equiv kE_{GW}(k)$  and the antisymmetric part,  $\Xi_{GW}(k)$ ; see

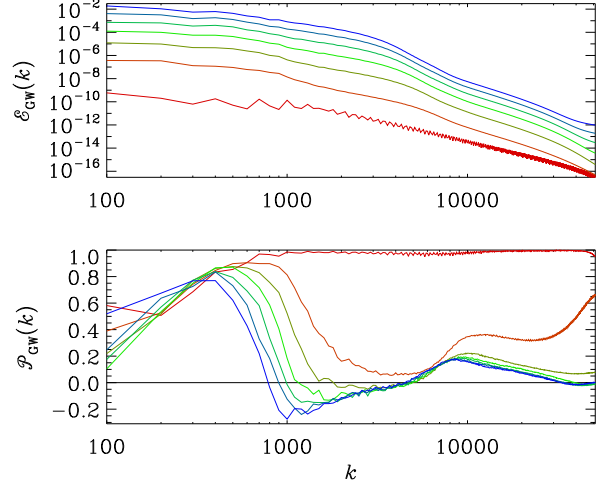


Figure 4: Same as Figure 3, but with  $n = 5$ .

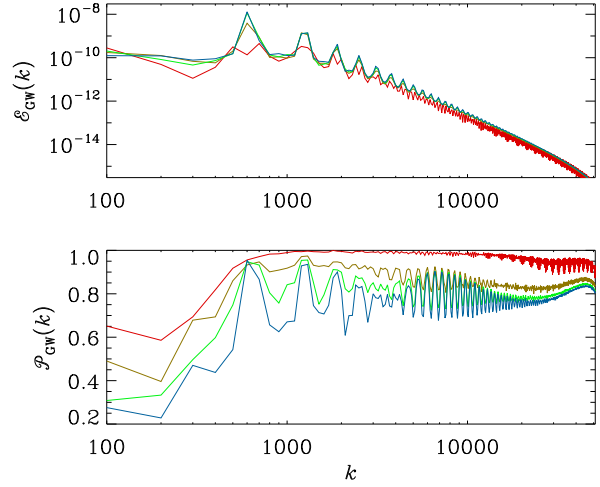


Figure 5: Same as Figure 3, but for a model of type B with  $\epsilon = 1$  and  $\tau = 0.01$ .

Ref. [18] for details. The reason is that at late times, the magnetic energy is so weak that it cannot change the GW spectrum noticeably. To get an idea of how small the effect is in comparison with the much larger effect of fluctuations, we now increase the value of  $n$  beyond  $n = 2/3$ . For  $n = 1$ ,  $E_{GW}$  grows by only 12%; so the results for  $n = 1$  and  $n = 2/3$  can hardly be distinguished from each other; see the lowermost red and black lines in Figure 1. For  $n = 2$ , for example, the value of  $E_{GW}(t)$  grows by a factor of  $\approx 30$  compared to the standard case, but  $E_{GW}(k, t)$  shows growth only at  $k > 2k_*$ .

Consequently, the dependence of polarization also only changes at small  $k$ ; see Figure 3. For  $n = 5$ , on the other hand, we see a clear growth at all  $k$ , and now  $\mathcal{P}(k)$  also declines rapidly at high  $k$ ; see Figure 4. Here, the GW energy grows obviously to unrealistically large values.

Finally, we consider models of type B. It turns out that now  $E_{\text{GW}}(k, t)$  increases preferentially only at discrete wave numbers,  $k = jk_*$ , with integers  $j \geq 1$ . The resulting polarization,  $\mathcal{P}_{\text{GW}}(k)$  increases more smoothly over the full range of wave numbers.

Our work has illuminated some of the more subtle aspects of turbulent GW production by time-dependent magnetic fields. Here, we have only considered the case of a given initial magnetic energy spectrum. This allowed us to produce a magnetic field that is fully helical at all wave numbers. In the other case of a driven initial spectrum, considered in Ref. [16], the fractional magnetic helicity declines to zero at higher wave numbers. This also happens in our present models with a given initial spectrum, but at those later times, the temporal fluctuations associated with the turbulence are too weak to have a noticeable effect. To illustrate this more clearly, we have artificially modified the time dependence of the stress by applying an  $F(t)$  function. Although the details between models of type A and B are different, they all have in common that the degree of circular polarization at  $k \gg 2k_*$  now decreases with time. However, our work also shows that, if the initial magnetic spectrum can indeed be assumed given as fully helical at all wave numbers, the degree of circular polarization at high wave numbers would indeed be close to 100%.

## References

- [1] T. Vachaspati 2001, PhRvL, 87, 251302
- [2] A. Díaz-Gil, J. García-Bellido, M. García Pérez and A. González-Arroyo 2008, PhRvL, 100, 241301
- [3] A. Brandenburg, T. Kahniashvili, S. Mandal, A. Roper Pol, A. G. Tevzadze, and T. Vachaspati 2017, PhRvD, 96, 123528
- [4] A. Neronov and I. Vovk 2010, Science, 328, 73
- [5] A. Brandenburg, K. Enqvist, and P. Olesen 1996, PhRvD, 54, 1291
- [6] M. Christensson, M. Hindmarsh, and A. Brandenburg 2001, Phys. Rev. E, 64, 056405
- [7] R. Banerjee and K. Jedamzik 2004, PhRvD, 70, 123003
- [8] A. Brandenburg, K. Subramanian 2005, A&A, 439, 835
- [9] The PENCIL CODE, <https://github.com/pencil-code>, DOI:10.5281/zenodo.2315093
- [10] A. Roper Pol, A. Brandenburg, T. Kahniashvili, A. Kosowsky, and S. Mandal 2020, Geophys. Astrophys. Fluid Dyn., 114, 130
- [11] T. Kahniashvili, G. Gogoberidze, and B. Ratra 2005, PhRvL, 95, 151301
- [12] L. Kisslinger and T. Kahniashvili 2015, PhRvD, 92, 043006 Polarized gravitational waves from cosmological phase transitions
- [13] A. Roper Pol, S. Mandal, A. Brandenburg, T. Kahniashvili, and A. Kosowsky 2019, PRD, submitted, arXiv:1903.08585
- [14] D. Biskamp and W.-C. Müller 1999, PhRvL, 83, 2195
- [15] A. Brandenburg and T. Kahniashvili 2017, PhRvL, 118, 055102
- [16] Roper Pol, A., Mandal, S., Brandenburg, A., Kahniashvili, T. and Kosowsky, A.
- [17] H. K. Moffatt 1978, Magnetic Field Generation in Electrically Conducting Fluids (Cambridge: Cambridge Univ. Press)
- [18] C. Caprini, R. Durrer, and T. Kahniashvili 2004, PhRvD, 69, 063006